PANSHI XIE*,**, YONGPING WU*,**

DEFORMATION AND FAILURE MECHANISMS AND SUPPORT STRUCTURE TECHNOLOGIES FOR GOAF-SIDE ENTRIES IN STEEP MULTIPLE SEAM MINING DISTURBANCES

MECHANIZMY POWSTAWANIA ODKSZTAŁCEŃ I PĘKANIA ORAZ TECHNOLOGIE WZMACNIANIA I ZABEZPIECZANIA ŚCIAN CHODNIKÓW W WYROBISKACH NACHYLONYCH

Entries in steeply pitching seams have a more complex stress environment than those in flat seams. This study targets techniques for maintaining the surrounding rock mass stability of entries in steep seams through a case study of a steep-seam entry at a mine in southern China. An in-depth study of the deformation and instability mechanisms of the entry is conducted, employing field measurement, physical simulation experiment, numerical simulation, and theoretical analysis. The study results show that the surrounding rock mass of the entry is characterised by asymmetrical stress distribution, deformation, and failure. Specifically, 1) the entry deformation is characterised by a pattern of floor heaving and roof subsidence; 2) broken rock zones in the two entry walls are larger than those in the roof and floor, and the broken rock zone in the seam-floor side wall is larger than that in the seam-roof side wall; 3) rock bolts in the middle-bottom part of the seam-floor side wall of the entry are prone to failure due to tensile stress; and 4) rock bolts in the seam-roof side wall experience relatively even load and relatively small tensile stress. Through analysis, disturbances were found to occur in both temporal and spatial dimensions. Specifically, in the initial mining stage, the asymmetrical rock structure and stress distribution cause entry deformation and instability; during multiple-seam multiple-panel mining operations, a wedge-shaped rock mass and a quasi-arc cut rock stratum formed in the mining space may cause subsidence in the seam-floor side wall of the entry and inter-stratum transpression, deformation, and instability of the entry roof and floor. The principles for controlling the stability of the surrounding rock mass of the entry are proposed. In addition, an improved asymmetrical coupled support structure design for the entry is proposed to demonstrate the effective control of entry deformation.

Keywords: steep seam group, goaf-side entry, asymmetrical deformation, arching effect, asymmetrical coupled support structure

Chodniki w wyrobiskach biegnących po upadzie charakteryzują się bardziej złożonym rozkładem naprężeń niż wyrobiska poziome. Celem niniejszej pracy jest zbadanie technik stabilizowania górotworu

---

*   SCHOOL OF ENERGY AND RESOURCE, XI'AN UNIVERSITY OF SCIENCE AND TECHNOLOGY, XI'AN 710054, CHINA
**   KEY LABORATORY OF WESTERN MINE EXPLOITATION AND HAZARD PREVENTION, MINISTRY OF EDUCATION, XI'AN 710054, CHINA

\#   Corresponding author: tay584@qq.com

562

w otoczeniu chodników nachylonych na podstawie studium przypadku chodnika o dużym stopniu nachylenia w jednej z kopalń w południowych regionach Chin. Przeprowadzono dogłębną i szczegółową analizę mechanizmów powstawania odkształceń i niestabilności w wyrobisku w oparciu o pomiary w terenie, eksperymenty w symulowanych warunkach fizycznych, symulacje numeryczne oraz analizy teoretyczne. Uzyskane wyniki wskazują, że górotwór w bezpośrednim otoczeniu chodnika charakteryzuje się asymetrycznym rozkładem naprężeń, odkształceń oraz pęknięć. W szczególności, analiza odkształceń wskazuje: 1) występowanie pęcznienia spągu oraz osiadania stropu, 2) strefy spękań skał w obydwu ścianach bocznych chodnika są większe niż strefy spękań w spągu i stropie, a strefa spękań w ścianie bocznej od strony spągu jest większa niż w pobliżu stropu; 3) podpory kotwiące w części środkowej ściany wyrobiska od strony spągu mają tendencje do pękania wskutek naprężeń rozciągających; 4) naprężenia działające na kotwy stabilizujące ścianę boczną chodnika w części bliżej stropu są stosunkowo równomierne, z kolei występujące naprężenia rozciągające są relatywnie niewielkie;

Analizy wykazały występowanie zaburzeń zarówno w ujęciu czasowym jak i przestrzennym. Na etapie rozpoczęcia prac wydobywczych odkształcenia i niestabilności chodnika powstają wskutek asymetrycznej struktury skał i asymetrycznego rozkładu naprężeń; w trakcie prac wydobywczych obejmujących wybieranie ścian w kilku polach powstają obszary warstw skalnych górotworu w kształcie klinów i łuków, co prowadzić może do osiadania ścian chodnika w pobliżu spągu, od strony wybieranego złoża, a także do zachodzenia na siebie warstw skalnych, odkształceń i niestabilności spągu i stropu w wyrobisku. W pracy zaproponowano zasady stabilizowania górotworu w otoczeniu wyrobiska. Ponadto, zaproponowano udoskonalony projekt zmodyfikowanego asymetrycznego wspornika podporowego do zainstalowania w chodniku, dla zademonstrowania skutecznej metody kontrolowania odkształceń wyrobisk chodnikowych.

Słowa kluczowe: wyrobiska chodnikowe nachylone, chodnik od strony zrobów, asymetryczne odkształcenia, efekt powstawania łuku, asymetryczny wspornik

1. Introduction

Coal plays an essential role in fuelling China's economic development, and the ratio of coal to primary energy consumption is projected to remain at approximately 50% until 2030 (National Development and Reform Commission, 2017). Steeply dipping coal seams (with dip angles exceeding 45°) constitute 10% of China's total coal reserves and 10% of China's total annual coal output. In southern China (for example, in Guizhou, Yunnan, and Sichuan Provinces), steep seams are present in 80% of coal mines, and most of these steep seams are quality coal resources (Wu et al., 2013). Therefore, recovering steep coal seams is very important to regional economic and social development in China.

However, considerable challenges are associated with the recovery of steep coal seams. Despite efforts to improve recovery methods, the control of the surrounding rock mass stability of gob-side entries remains a key problem. As demonstrated by extensive research and practice (Wang et al., 2016; Deng et al., 2014; Frumkin et al., 1983; Ladenko et al., 1974; Tu et al., 2017; Wu et al., 2001; Huang et al., 2004; Hou et al., 2001; Zheng et al., 2014 and Ma et al., 2016), compared with flat seams, steep seams pose additional challenges with regard to entry stability control due to the widely differing occurrence conditions and lithological properties of the surrounding rock mass. In particular, for an entry in a steep seam, the two sidewalls correspond to the seam roof and floor, while large parts of the roof and floor comprise the seam. Furthermore, well-developed joints and cracks occur, yielding poor entry structure strength. Under the impact of mining disturbances, the deformation and failure behaviours of entries in steep seams are more complex than those in flat seams.

In this study, an in-depth analysis of the deformation and failure mechanisms of entries in steep seams is conducted, with the aim of improving entry support structure design to main-

tain entry stability against disturbances caused by multiple mining activities, and to provide a scientific criterion for handling challenges associated with entry support structures in steep seams. To this end, a case study of a soft rock entry at a mine located in Sichuan Province, China is conducted. The case study is performed by reviewing existing engineering practices and employing field measurement, physical simulation experiments, numerical simulation, and theoretical analysis.

2. Case Study

2.1. Mining site engineering conditions

The Zhaojiaba Mine in Guangwang Mining District, Sichuan Province, is characterised by complex geological conditions. There are three recoverable seams at the mine: No. 8-10 from the top to the bottom, all with dip angles exceeding 55° and small inter-seam distances; the distance between seams No. 9 and 10 is approximately 2 m (Fig. 1). In accordance with the seam occurrence conditions and available mining technology, flexible shield support and pitching oblique mining have been adopted at the mine. Specifically, panels in the same district (including seams No. 8-10) have been mined out from the top to the bottom, and a gob-side entry retention system has been implemented for retreat mining, where the head entry of the mined-out panel is used as the return airway for the next panel in the same seam. Panel No. 3964 in district No. 306 – the subject of this case study – is located in seam No. 9, with an inclined working face of 80 m, strike of 360 m, and average dip angle of 64°, as shown in Fig. 1. The entry of panel No. 3964 is located at the downside panel at level +340, which serves as the head entry of panel No. 3964 and as the return airway of the downstream adjacent panel, No. 3966. The entry has an isosceles trapezoid cross-section, with a net height of 2.4 m and width of 3.0 m. The entry is supported by an I-steel shed structure, with the voids in the roof shielded with wood panels.

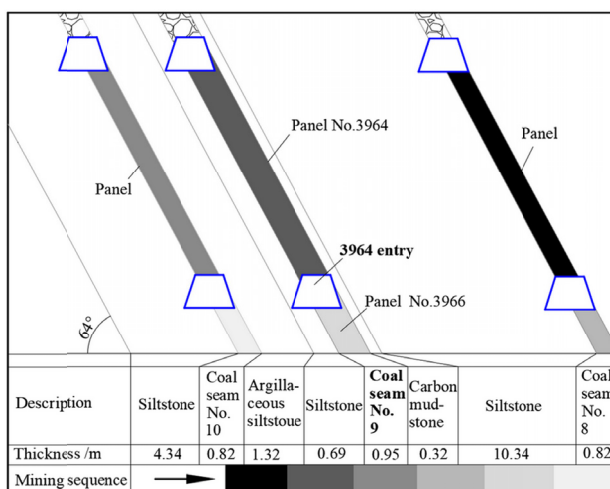| Description	Siltstone	Coal seam No. 10	Argilla-ceous siltstoue	Siltstone	Coal seam No. 9	Carbon mud-stone	Siltstone	Coal seam No. 8
Thickness /m	4.34	0.82	1.32	0.69	0.95	0.32	10.34	0.82
Mining sequence	→							

Fig. 1. Lithological characteristics and mining layout of Panel No. 3964

The surrounding rock mass of the entry is a half-coal-half-rock structure, with a buried depth of approximately 600 m and well-developed beddings and joints, as well as many partings in the seam (Fig. 2a). Both the seam roof and floor are composed of a geological structure of soft, weak argillaceous and carbonaceous rocks. The distance between the entry floor and seam No. 10 is small, at only 1.32 m. The entry is of a gob-side entry retention design, intended as a long-life structure to serve both the adjacent panels in succession. The entry is subject to multiple mining disturbances: disturbances due to the mining activities in both the adjacent panels in seam No. 9, as well as those generated by the mining activities in seams No. 8 and 10.

2.2. Entry deformation and failure characteristics

As shown in Fig. 2b, the entry of panel No. 3964 was severely deformed during entry driving and panel production. As observed on-site, the deformation began at the floor, manifesting as floor heaving, then induced wall-feet instability, and finally caused roof subsidence; the I-beam feet of the shed support at the seam-floor side was severely bent, twisted, and deeply penetrating the floor. The deformation was asymmetrical and characterised by floor heaving and roof subsidence, and the entry cross-sectional shape changed from a trapezoid to an irregular quadrangle. The local convergence in some areas of the roof was up to approximately 1 m when mining panel No. 3966, as shown in Fig. 2c. The deformed entry necessitated multiple and highly frequent repairs to maintain the minimum stability level; this incurred high maintenance costs and severely affected the normal production operations of the panel (Zhang, 2014).
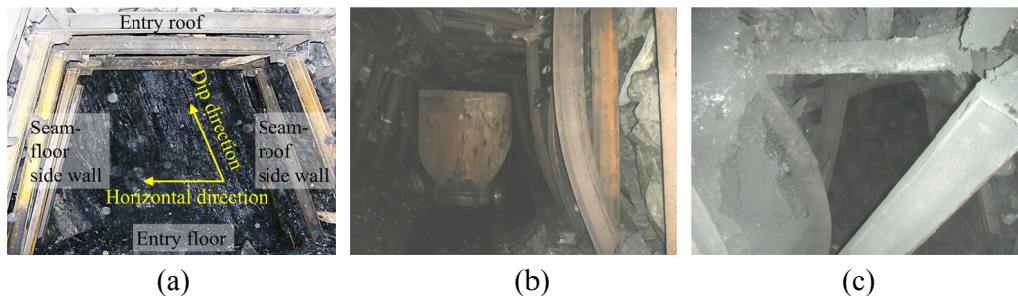

(a) (b) (c)

Fig. 2. Deformation and failure characteristics of panel No. 3964 entry during different stages of mining operation: (a) Initial stage of entry driving, (b) mined-out panel No. 3964, and (c) mined-out panel No. 3966 (adjacent to No. 3964)

3. Measuring Broken Rock Zones in Entry Surrounding Rock Mass

The surrounding rock mass of the entry was investigated for broken rock zones using a SIR-20 multichannel ground-penetrating radar data acquisition unit (Geophysical Survey Systems, Inc.) in conjunction with a 100-MHz antenna with 12-m detection depth. Eight measurement points spaced at 10-15 m were established along the entry, with four test leads for each testing point to cover the floor, seam-floor side wall, roof, and seam-roof side wall. These sections are shown in Fig. 2a.

The resulting waveforms generated by the radar device were then analysed. A clear bend in the waveform indicates a broken rock zone in the surrounding rock mass, whereas an irregularity in the vertical waveform pattern indicates cracking or manifestation of a structural failure (Wang et al., 2013). Based on an on-site investigation and analysis of the obtained measurement data, the broken rock zones were found to differ at different measurement points and at different locations near the same measurement point. Fig. 3 shows the results obtained from measurement point No. 7, which is located 40 m away from the panel face. A clear bend at a depth of 5.2 m in the waveforms of the entry floor (Fig. 3a) is apparent, indicating a stable rock-broken rock interface in the surrounding rock mass. A bend at a depth of approximately 2.5 m is apparent in the waveforms obtained by each of the other three test leads (Figs. 3b-d).
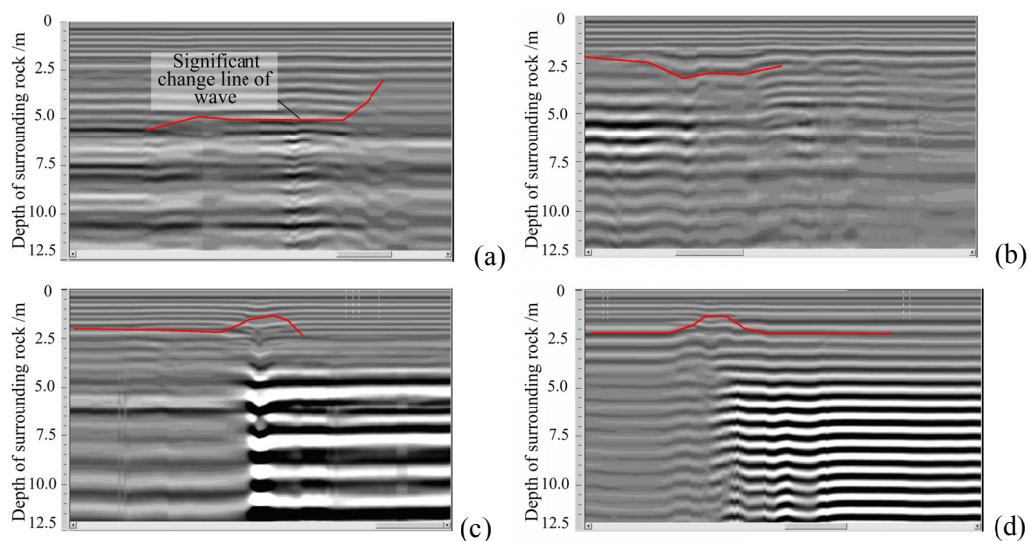
Fig. 3. Waveforms obtained from measurement point No. 7 using ground-penetrating radar, for entry (a) floor, (b) seam-floor side wall, (c) roof, and (d) seam-roof side wall

Based on the broken rock zones in the surrounding rock mass of panel No. 3964 entry identified through measurement, as well as the occurrence conditions and convergence of the surrounding rock mass observed on-site, the breaking characteristics of the surrounding rock mass were graphically represented as a broken contour, as shown in Fig. 4. This figure shows six broken rock zones greater than 4.0 m in size. The size of the broken-rock-zone showed ranges of 1.4-5.2 m in the entry floor (test lead No. 1), 1.8-4.5 m in the seam-floor side wall (test lead No. 2); 1.5-4.0 m in the roof (test lead No. 3), and 1.8-4.1 m in the seam-roof side wall (test lead No. 4). Generally, the broken contour of the surrounding rock mass is asymmetrical, with larger broken rock zones in the two entry walls than in the roof and floor, and a larger broken rock zone in the seam-floor side wall than in the seam-roof side wall. In addition, the broken rock zones identified through measurement are consistent with the convergence characteristics of the surrounding rock mass observed on-site. Based on the theory of broken rock zones in the surrounding rock proposed by Dong et al. (1994), the majority of the surrounding rock mass

can be classified as type-V unstable surrounding rock with a large broken rock zone. However, the surrounding rock near the seam-floor side wall can be classified as type-VI very unstable surrounding rock with a large broken rock zone. Based on the above classifications as well as the tested lithological properties of the surrounding rock mass (Table 1), the surrounding rock of the entry can be classified as fractured soft rock.

4. Design and Testing of Entry Cross-sectional Geometry and Support Structure

4.1. Design of entry cross-sectional geometry and support structure

The cross-sectional geometry of the entries was designed based on: a) the nature of the broken zone measurement results, b) deformation and failure characteristics of the entry, and c) good structure and integrity of the immediate roof of the coal seam in the vicinity of seam No. 9. The cross-sectional geometries of the entries have an inclined straight wall at the seam-roof side (siltstone immediate roof) measuring 2.6 m in length; an arc wall at the other side and an arc roof with radii of 4.3 and 1.5 m, respectively; and entry measurements of 2.5 m in height and 3.4 m in width at the floor.

Based on the existing support structure design, surrounding rock mass deformation observed on-site, and broken-rock-zone measurement results, an asymmetrical support structure design coupling high-strength rock bolts, wire mesh, and anchor cable was adopted for the panel No. 3964 entry. The two walls and roof of the entry were supported with nine screw-thread steel rock bolts (Φ18 mm × 2000 mm high strength, left-turning thread, without longitudinal rib). The seam-floor side of the floor was supported with two screw-thread steel rock bolts (Φ18 mm × 1800 mm high strength, left-turning thread, without longitudinal rib). Each row was configured with 11 bolts, spaced 800 × 800 mm, and the bolt support plate measured 180 mm in length, 180 mm in width, and 10 mm in thickness. The bolting structure was reinforced with W-steel straps
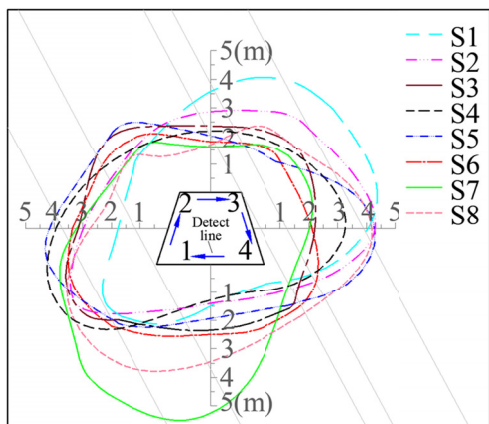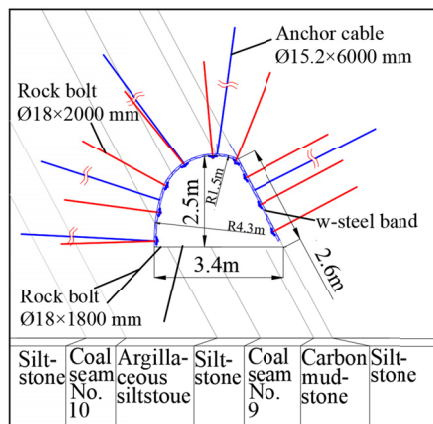

Fig. 4. Broken contour of surrounding-rocks

Fig. 5. Entry cross-sectional design and support structure

and diamond-shaped wire meshes. The anchor cable specifications were Φ15.2 mm $\times$ 6000 mm twin wire, cage type, and the cables were spaced at 1000 $\times$ 3200 mm, as shown in Fig. 5.

4.2. Simulation experiment for entry support structure

A simulation experiment examining the entry deformation and failure was performed on a physical simulation bench capable of two- and three-dimensional confining pressure loading and real-time load testing. Based on the occurrence conditions of the surrounding rock mass (Fig. 1) and the tested lithological-physical properties of the coal and rock (Table 1), a model with a geometrical similarity ratio of 1:10 was constructed, which measured 1500 mm in length, 600 mm in thickness, and 1500 mm in height, as shown in Fig. 6. The proportion of similar materials in different rock layers was determined according to the similarity principle (Li, 1994). River sand was selected as an aggregate for similar materials, and gypsum and calcium carbonate were used as bonding materials. The average bulk density of the materials was 1600 kg/m^3. The materials were mixed according to the determined proportion, mixed with appropriate amounts of water, and then the model was designed, with 20 tons of mica as the layered material between rock layers. The simulation experiment was conducted after the model was completely dried. The model was connected to testing and measuring instruments necessary for real-time monitoring of the deformation and pressure of the surrounding rock mass, as well as the stresses experienced by the rock bolts.

TABLE 1

Physical-mechanical properties of coal and rock

Serial no.	Lithological description	Unit weight (kg/m^3)	Elasticity modulus (MPa)	Poisson ratio	Tensile strength (MPa)	Cohesion (MPa)	Angle of internal friction, (°)
1	Carbonaceous mudstone	2610	3601	0.30	1.15	1.20	26.20
2	Siltstone	2640	6310	0.31	2.27	2.79	37.82
3	Coal	1450	3520	0.32	0.89	1.25	25.12
4	Argillaceous siltstone	2640	6310	0.31	2.27	2.79	37.82

Vertical and lateral loads were simultaneously applied to the model. At 5-MPa pressure, the deformation rate of the surrounding rock began to increase, with relatively large deformation in the entry floor and seam-floor side wall. The deformation and failure of the surrounding rock that developed along the direction of the seam dip angle was monitored. At 15-MPa pressure, failure of the coal seam occurred in the entry roof and floor as well as in the seam-floor side wall; specifically, transpression failure occurred in the entry roof owing to slipping and squeezing of the rock strata on both sides, as well clear heaving in the seam-floor side of the floor, as shown in Fig. 7.

Throughout the experiment, the model was monitored for entry surface displacement using an optical total station and dial gauges. The entry surface displacement gradually increased with an increase in the confining pressure, as shown in Fig. 8a. The order of monitoring entry deformation rate and its magnitude was undertaken with respect to the seam as follows, from high to low: the seam-floor side wall, floor and seam-roof side wall, and roof. The maximum accumulative convergence in the roof and floor was 0.15 m and 0.6 m in the two entry walls. In addition, the monitored displacement of the surrounding rock exceeded 2 m, with the largest
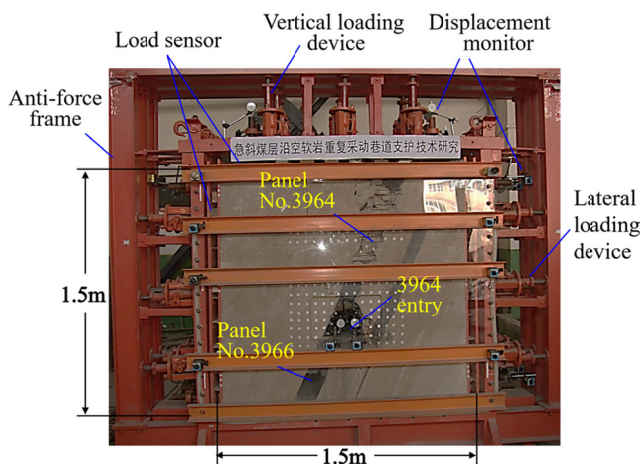
Fig. 6. Physical simulation model on simulation bench capable of two-dimensional and three-dimensional loading
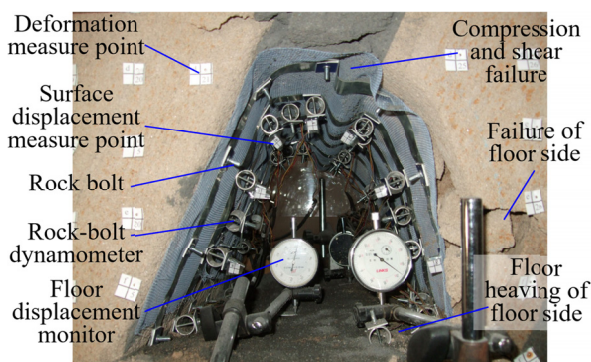

Fig. 7. Physical simulation experiment results of panel No. 3964 entry

displacement occurring for the seam-floor side wall, at 3-4 m (Fig. 8b). The rock displacement in the roof was approximately 2-3 m, which was basically consistent with the broken-rock-zone measurement results.

Throughout the physical simulation experiment, the stresses experienced by the rock bolts (initial force: 50 kN) were monitored using a load cell, as shown in Fig. 9. The monitored results indicate that the rock bolts located in different cross-sectional areas of the entry model experienced different stresses. The rock bolts in the seam-floor side wall experienced the greatest axial stress, with a maximum value of 213.4 kN, followed by the bolts in the floor, with a maximum value of 119.6 kN. The maximum axial stress experienced by the bolts in the seam-roof side wall was 105.0 kN. Finally, the bolts in the roof experienced the smallest axial stress, with a maximum value of 99.6 kN. The uneven stresses experienced by the bolting structure can be attributed to the uneven deformation distribution shown in Fig. 8a. The largest deformation occurred for the seam-floor side wall; thus, the rock bolts in that location experienced high tensile stress. The deformation
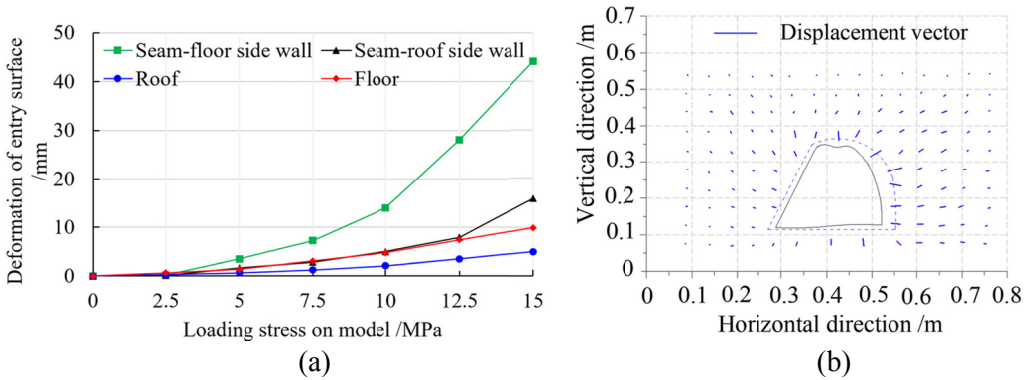
Fig. 8. Deformation and failure characteristics of entry surrounding rock mass:
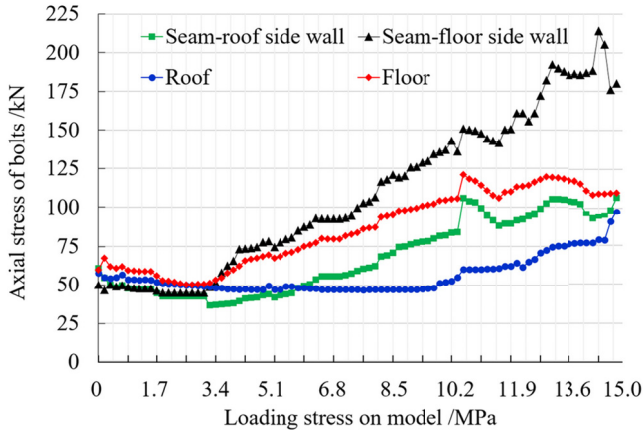(a) Surface deformation and (b) displacement characteristics

Fig. 9. Axial stress curves of rock bolts

of a similar magnitude occurred for the seam-floor side of the floor; thus, the rock bolts in that location also experienced high axial stress. The seam-roof side wall had high-strength surrounding rocks and good structural integrity, and it could buffer the stress; hence, smaller deformation occurred and the rock bolts in that location experienced relatively even load and small axial stress.

5. Entry Deformation and Instability Mechanisms under Disturbance from Multiple Mining Activities

5.1. Asymmetrical deformation and failure

Based on a comprehensive analysis of the broken-rock-zone measurement, the physical simulation experiment, and numerical simulation results, it was determined that the entry sta-

bility is threatened by multiple disturbances in both the temporal and spatial dimensions. The stress distribution in the surrounding rock mass is uneven owing to the attitude and lithological properties of the surrounding rock mass. Furthermore, the numerical simulation results showed that the initial stress in the entry roof exceeded that in the entry floor, as the roof was a siltstone mass with good structural integrity, high strength, and good anti-deformation capacity, whereas the floor is an argillaceous siltstone mass with well-developed joints and low strength. As a result, in the initial stage of entry driving, the entry floor heaved, and large deformation occurred in the seam-floor side wall of the entry, whereas relatively small deformations occurred in the other areas of the surrounding rock mass. Thus, an overall asymmetrical deformation was clearly established, as shown in Fig. 10a.

When seam No. 8 was mined out (see Fig. 1), the entry experienced a second disturbance. Meanwhile, the initial stress in the roof of seam No. 9 (the floor of seam No. 8) released, or the entry simultaneously experienced the disturbance resulting from the stress release, thereby aggravating the asymmetrical deformation in the two entry walls. The mining of panel No. 3964 (the third mining disturbance) caused a release of the stress around the working face, thereby alleviating the deformation in the entry roof. This phenomenon was consistent with the physical simulation experiment results, but the stress field in the surrounding rock mass was still clearly characterised by an asymmetrical distribution, as shown in Fig. 10b.
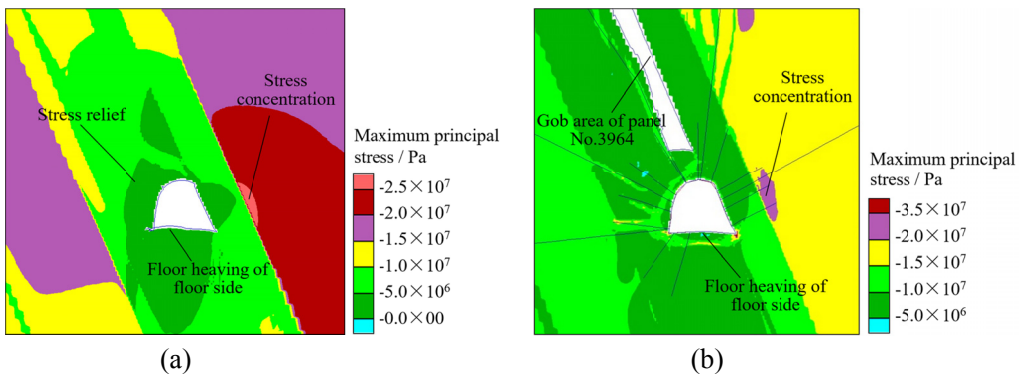

Fig. 10. Asymmetrical mechanical characteristics of entry at different mining stages: (a) entry driving and (b) panel No. 3964 mined out

5.2. Wedging and arching effect

While panel No. 3964 was being mined out, the roof and floor of the mined-out area were displaced towards the stopped-out space, yielding reduced cohesion between the entry floor and seam No. 10. Consequently, the siltstone stratum became a long, large, inclined, wedge-shaped body, which slipped downward along seam No. 10 under the effect of gravity, exerting pressure on the seam-floor side wall of the entry and causing local deformation. There was greater deformation in the area nearer to the bottom of the wedge-shaped body, as shown in Fig. 11.

While the panels upstream and downstream of the panel No. 3964 entry were being mined out, the roof of the mined-out area caved in, yielding an arch-shaped cross-section for the gob roof. The surrounding rock at the upstream and downstream entries serve as the two feet of these

arches and the caved-in roof of the mined-out area constitutes the arch body (Shi, 1999). This was the fourth mining disturbance, which induced transpression and slipping of the entry roof and floor and finally caused the small coal body at the entry roof to break, as shown in Fig. 12.
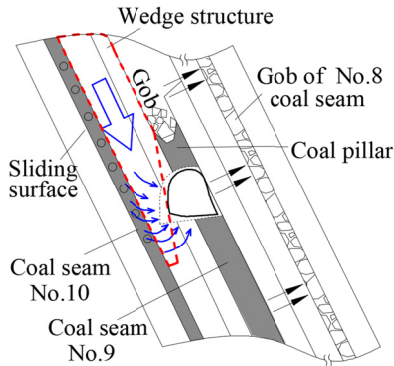
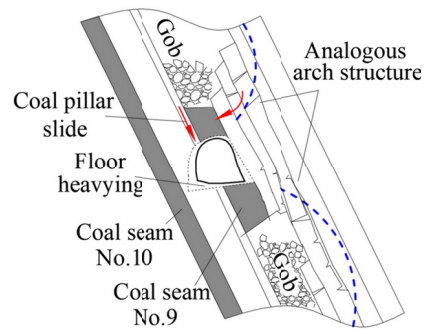Fig. 11. Wedging effect on entry instability due to mining operations in upstream panel

Fig. 12. Arching effect on entry instability due to mining operations in downstream panel

6. Improved Bolt-Mesh-Cable Entry Support Structure and Implementation Results for Improved Design

Based on the above analysis of the entry instability mechanism under the impact of multiple disturbances, the root cause of the instability of the softrock gob-side entry is believed to be the asymmetrical load of the surrounding rock mass on the support structure. Therefore, it was necessary to fully utilise the support capacity of a rock bolt-wired mesh-anchor cable support structure in accordance with the uneven load distribution in the surrounding rock of the entry. This allowed a more even stress distribution in the surrounding rock mass, with more harmonious deformation of the support structure and surrounding rock mass. In addition, it ensured the stability of the latter. Considering the above, the following principles for controlling the stability of the surrounding rock mass of the entry were proposed: active support, additional reinforcement at critical points, and coupled support. Improvement of the existing support structure by an asymmetrical support structure design coupling high-strength rock bolts, long anchor cables, W-steel straps, and steel-bar meshes was proposed. The design parameters are detailed below.

(1) Rock bolts: spaced at 800 mm × 800 mm 12 bolts per grille (four in the roof, all perpendicular to the roof, three in each wall, with the middle bolt perpendicular to the wall; two on the seam-floor side of the floor). Material specifications: $\Phi20$ mm× 2500 mm (2200 mm for the two bolts on the seam-floor side of the floor), high-strength screw-thread steel, left-turning thread, equal strength along the total length, initial compression exceeding 50 kN. Rock-bolt supporting plate: 200 mm × 200 mm × 20 mm (length × width × thickness). Each bolt grille was reinforced with three high-strength W-steel straps and joined with a lap length exceeding 200 mm.

(2) Anchor cables: material specifications: $\Phi17.8$ mm × 7000 mm, twin wire, cage type; one in the middle of the roof; one in the middle of the seam-roof side wall; one each in the top, middle, and bottom of the seam-floor side wall; spaced 1000 mm × 3200 mm.

(3) Wire mesh: material specifications: #10 galvanised wire; dimensions: 2000 mm × 1000 mm for the two walls, 4100 mm × 1000 mm for the roof; mesh size: 80 mm × 80 mm; joined mesh-by-mesh with a lap length of 200 mm.

A field test of the improved support structure design for the entry was conducted, as shown in Fig. 13a. The monitored field results show that the entry remained stable, as demonstrated by the magnitude of the convergence of the two walls, roof, and floor measured on the 30th (experiencing the second mining disturbance) and 48th day (experiencing the third mining disturbance) after implementation. The maximum rib-rib and floor-roof convergences were 112 and 122 mm, respectively; the maximum convergence rates were 7.02 and 10.63 mm/d, respectively, and the minimum convergence rate was 0.35 mm/d, as shown in Fig. 13b. The deformation in the walls was clearly reduced, demonstrating a clear effect of the improved design, and the deformation in the roof and floor was also reduced to some degree, thereby providing a basic guarantee of entry stability. With the implemented rock bolt-wire mesh-anchor cable asymmetrical support system, the deformation rate was increased in the initial stage. When the upstream and downstream panels were being mined out, the rib-rib convergence rate gradually decreased and severe deformation of the surrounding rock was effectively curtailed. Therefore, repair was no longer needed to maintain the entry stability level during the multiple mining disturbances; furthermore, the maintenance cost of the entry was largely reduced, thereby ensuring that normal mining operations could be performed.
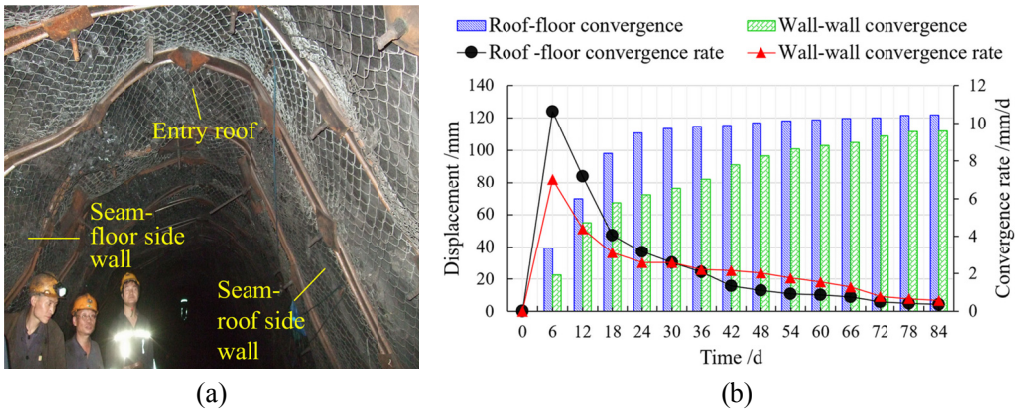

Fig. 13. (a) Improved support structure design for entry of panel No. 3964 and (b) monitored results of entry deformation after implementation of the improved design

Furthermore, the improved bolt-mesh-cable entry support structure is also applied to the gob-side entry of the steep coal seam at the Daichiba Mine, Tangdong Mine, and Tangjiahe Mine, and the results demonstrated effective control of entry deformation during the mining process of the panel. Field implementation results also show that the roadway support optimization scheme greatly reduces the maintenance efforts of the mining entry, while ensuring safe and normal production of the mine with obvious economic benefits.

7. Conclusions

An in-depth study of the deformation and failure mechanisms of an entry in a steep seam at Zhaojiaba Coal Mine was conducted, in which the broken rock zones in the surrounding rock mass of the original entry were measured, the entry support structure was redesigned based on the results of a preliminary physical simulation experiment and numerical simulation, and the improved design was implemented and monitored. Our research conclusions can be summarised as follows:

(1) The entry was special in terms of its half-coal-half-rock structure, complex stress distributions in the surrounding rock mass, and multiple mining disturbances. The entry deformation was characterised by an asymmetrical pattern. The floor heaved, and the roof subsided; as a result, the seam-floor side feet of the shed support structure were severely bent and twisted, and deeply penetrated the floor.

(2) The broken rock zones in the surrounding rock mass of the entry were characterised by an asymmetrical distribution. The broken rock zones in the two entry walls exceeded those of the entry roof and floor, and the broken rock zone in the seam-floor side wall was greater than that in the seam-roof side wall. The majority of the surrounding rock mass of the entry could be classified as type-V unstable surrounding rock with a large broken rock zone, and the surrounding rock near the seam-floor side wall of the entry could be classified as type-VI very unstable surrounding rock with a large broken rock zone. In general, the surrounding rock of the entry could be classified as fractured soft rock.

(3) An improved support structure was proposed, with an asymmetrical structural design consisting of rock bolts, wire meshes, and anchor cables. The physical simulation experiment demonstrated that the unique cross-sectional design (an inclined straight wall on one side, an arc wall on the other side, and an arc roof) well suited the unique site conditions. That is, transpression failure occurred for the coal mass in the entry roof owing to the slipping and squeezing of the rock masses on the two sides, and clear heaving occurring on the seam-floor side of the floor. The rock bolts experienced uneven pressure, with the bolts on the seam-floor side wall experiencing high tensile stress due to the large deformation in that area. The bolts on the seam-floor side of the floor experienced high axial stress due to floor heaving in that area. In contrast, the bolts on the seam-roof side wall experienced a relatively even load and smaller tensile stress because of their high strength, good structural integrity, and relatively small deformation of the surrounding rock at that location.

(4) The deformation and failure mechanisms of the gob-side entry were very complex because of the disturbances in both the temporal and spatial dimensions. In the initial mining stage, the asymmetrical rock structure and stress distribution caused entry deformation and instability. During the occurrence of multiple-seam multiple-panel mining operations, or when the entry experienced multiple mining disturbances, a wedge-shaped rock mass and a quasi-arc rock stratum were formed in the mining space. These wedging and arching effects in the surrounding rock mass of the entry resulted in the subsidence of the seam-floor side wall and inter-stratum transpression, deformation, and instability of the roof and floor.

(5) The following principles for controlling the stability of the surrounding rock mass of the entry were proposed: active support, additional reinforcement at critical points, and coupled sup-

574

port. An improved support structure design for the entry was also proposed, i.e. an asymmetrical structure coupling high-strength rock bolts, long anchor cables, W-steel straps, and steel-bar meshes. Field implementation results show that the improved design enabled effective control of the surrounding rock mass deformation and met safe production requirements.

Acknowledgements

References

Deng Y.H., Wang S.Q., 2014. *Feasibility analysis of gob-side entry retaining on a working face in a steep coal seam*. International Journal Mining Science and Technology **42**, 4, 499-503.

Dong F.T., Song H.W., Guo Z.H., 1994. *Theory of rock broken zone in roadway*. Journal of China Coal Society **19**, 1, 21-31 (in Chinese).

Frumkin R.A., Podtikalov A.S., 1983. *Predicting rock behaviour in steep seam faces*. International Journal Rock Mechanics of Mining Science *&* Geomechanics Abstracts **20**, 1, a12-a13 (in Russian).

Hou C.J., Bai J.B., Zhang N., Li H.Y., 2001. *Coal roadway bolting under difficult and complex conditions*. Journal of Geotechnical Engineering **23**, 1, 84-88(in Chinese).

Huang Q.X., 2004. *Support measures and mine pressure in steep critical angle coal seam along gob-side entry*. Journal Mining Pressure and Roof Control **21**, 4, 44-46(in Chinese).

Ladenko A.A., 1974. *Improvements in working steep seams*. International Journal Rock Mechanics of Mining Science *&* Geomechanics Abstracts **11**, 12, 247(in Russian).

Li H.C.,1994. *Mine pressure simulation experiment.* China University of Mining and Technology Press, 2-10 (in Chinese).

Ma Z.Q., Jiang Y.D., Yang Y.M., 2016. *Deformation characteristics and control technology of roadway in steep and soft coal seam*. Journal of Mining and Safety Engineering **33**, 2, 253-259(in Chinese).

National Development and Reform Commission, 2017. *The 13th five-year development plan for China's coal industry*, (in Chinese).

Shi P.W., 1999. *The complexity of the movement of old roof crack in steep coal seam*. Journal Mining Pressure and Roof Control **3**, 4, 26-28 (in Chinese).

Tu H.S., Tu S.H., Zhang C., Zhang L., Zhang X.G., 2017. *Characteristics of the Roof Behaviours and mine pressure manifestations during the mining of steep coal seam*. Archives of Mining Sciences **62**, 4, 871-890.

Wang J.A., Jiao J.L., 2016. *Criteria of support stability in mining of steeply inclined thick coal seam*. International Journal Rock Mechanics of Mining Science **82**, 2, 22-35.

Wang N.B., Cao J.T., Lai X.P., 2013. *Characteristics of stope migration and roadway surrounding rock fracture for fully mechanized top coal caving face in steeply dipping and extra thick coal seam*. Journal of China Coal Society **38**, 8, 1312-1318(in Chinese).

Wu Y.P., 2001. *Asymmetric loading effect in entry (tunnel) support*. Journal Xi 'an Jiaotong University **40**, 2, 55-57(in Chinese).

Wu Y.P., Xie P.S., Wang H.W., Yun D.F., Ren S.G., Chen X.K., 2013. *Theory and practice of fully mechanized longwall mining in steeply dipping coal seams*. Mining Engineerin **65**, 1, 35-41.

Zhang Y.T., 2014. *Deformation characteristics and support technology of roadway surround rock in steep coal seam* [Master's Thesis], Xi'an University of Science and Technology (in Chinese).

Zheng P.Q., Chen, W.Z., Yuan J.Q., 2014. *Improvement of supporting parameters of inclined roadway in deep steep coal seam*. Rock and Soil Mechanics **35**, S2, 429-436 (in Chinese).